Investigated charge carrier effects in silicon membranes using a femtosecond laser

WI Ndebeka[1], PH Neethling[1], CM Steenkamp[1], H Stafast[1,2], EG Rohwer[1]

[1] Laser Research Institute, Physics Department, Stellenbosch University, PO Bag X1, Matieland 7602, South Africa

[2] Leibniz Institute of Photonic Technology, Albert-Einstein-Str. 9, 07745 Jena, Germany

E-mail: ndebeka@sun.ac.za

Abstract. The second harmonic (SH) generated at the Si/SiO_2 interface varies on a time scale of several seconds when illuminated with high intensity near infrared laser pulse trains (λ = 800 nm, 80 fs, 80 MHz repetition rate, $E_{pulse} \leq$ 10 nJ). The temporal behaviour arises from generation of trap sites and subsequent trapping of charges at the interface via multi-photon processes. These trapped charges create an interfacial electric field which influences the nonlinear properties of the Si/SiO_2 interface and leads to a time dependent second harmonic (TDSH) signal under continuous irradiation. This is known as electric field induced second harmonic (EFISH) generation. In this work, measurements are focused on the simultaneous measurements of EFISH signal from a free standing oxidized Si membrane both in reflection and transmission as a function of the irradiation time. Results show that the transmission of the fundamental irradiation as well as the transmitted SH signal generated from the Si membrane increases, reaches a maximum, and then decreases again as the input intensity is increased. The nonlinear behaviour of the transmitted signal is explained using free charge carrier absorption (FCA) in silicon.

1. Introduction

The silicon-silicon dioxide (Si/SiO_2) interface has been one of the most studied systems in the realms of materials and condensed matter physics. Despite the great outpouring of research and the huge commercial success, there has been little effort to construct a comprehensive, unified microphysical model of the Si/SiO_2 system [1-3]. The optical properties, both linear and nonlinear, of the interface region which are of interest, since this transition region varies considerably from those of the adjacent bulk phases. The second harmonic (SH) generation is used as a versatile tool to investigate buried surfaces and interfaces of centrosymmetric material, in which the electric field induced second harmonic (EFISH) generation processes is used as a valuable technique to investigate the mechanisms of charge transfer and trap generation [5 - 7]. The time dependence of the resulting EFISH signal is a measure of the rate of trap site generation and population, by both electrons and holes being pumped across the interface [8]. In this work, simultaneous time-dependent second harmonic (TDSH) measurements in reflection from and transmission through a Si membrane are presented. The transmission and reflection of the fundamental laser power are also measured and discussed using free carrier absorption (FCA) in silicon.

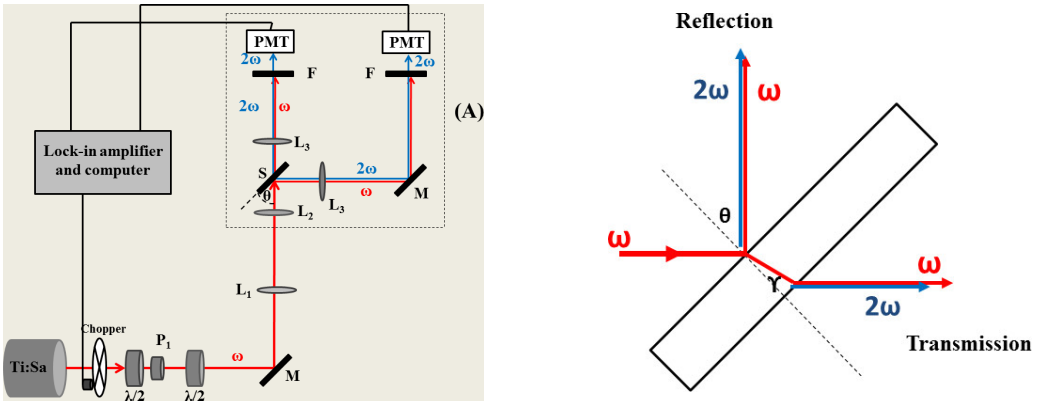

(a) (b)

Figure 1: (a) Schematic diagram of the EFISH setup used during this study. (b) Laser beam reflection from and transmission through thin Si membranes; external angle of incidence $\theta = 45\,^{\circ}$; within silicon $\gamma \approx 11\,^{\circ}$. ω and 2ω are the fundamental and SH signals, respectively.

2. Experiments

The optical source used in this work is a titanium-doped sapphire femtosecond laser oscillator (Spectra Physics, 3941-M3S, tsunami) capable of tunable laser operation over a broad range of near infrared (NIR) wavelengths. The femtosecond laser is pumped by a frequency doubled Nd:YVO_2 laser (Spectra Physics, Millenia V) with 5.5 W continuous wave (cw) maximum power output at a wavelength of 532 nm [9]. Figure 1a shows the schematic diagram of the experimental setup used in this work. The p-polarized beam from the Ti:Sapphire laser ($\lambda_c = 800\,\text{nm}$, $\tau = 80\,\text{fs}$ at 80 MHz repetition rate) passes through a half wave plate, $\lambda/2$, and a polarizer for power adjustment. The polarized beam is then incident on the sample, after being guided by a set of silver mirrors, collimated and focused by two lenses, L_1 and L_2, respectively. Light is incident on the sample at an external angle of $45\,^{\circ}$. The incident laser light is focused down to 11 μm diameter on the sample surface. The focal plane position is determined by a z-scan like measurement meaning that the sample is moved along the incident laser beam through the beam focus and the generated SH intensity is measured as a function of the sample position z. The fundamental laser beam has a Gaussian spatial beam profile. The Rayleigh length of the focus is $z_R = 5.57\,\mu\text{m}$ is obtained by fitting the SH intensity with the following expression [10]:

$$P_{2\omega} = \frac{K}{1 + z^2/z_R^2}, \tag{1}$$

with $K = (\eta P_\omega^2)/(\pi w_0^2)$. Here P_ω and $P_{2\omega}$ are the fundamental incident and SH converted powers, respectively, η is the SH conversion efficiency constant and $w_0 = w(z = 0)$, with $w(z)$ being the radius of the incident beam of frequency w at a position z along the propagation direction. For both the transmitted and reflected beams, the fundamental and SH light are collimated by identical lenses L_3. A power meter is used to measure the fundamental transmitted and reflected powers. For the power measurements, no filter is used to block the SH light generated on the sample as its contribution to the measurements is negligibly small. For the time-dependent second harmonic (TDSH) measurements, two identical filters, F were used to allow the SH light to pass through while blocking the transmitted and reflected fundamental beams.

The detection of the SH signals were done by use of two identical photomultiplier tubes, PMT. To enhance the signal-to-noise ratio, the SH signals measured in transmission and in reflection are amplified by a digital lock-in amplifier, with 2 physical units, in combination with a 500 Hz light

chopper. The lock-in amplifier, with LabView software, was connected to a computer for data acquisition. The samples were prepared from commercial ⟨100⟩-Si wafers by chemical etching using tetramethylammonium hydroxide (TMAH) to produce thin membranes of $3 \times 3\,\mathrm{mm}^2$ area with different thicknesses [13]. The wafers are slightly p-doped ($3 - 6 \times 10^{14}\,/\mathrm{cm}^3$). Before the investigations, the samples are cleaned using acetone and hydrofluoric acid to remove dirt and old oxide layers, respectively. In contact with air, the clean surfaces oxidize under dark room conditions reaching an equilibrium thickness of ($< 5 \pm 0.5$) nm within 48 hours [11].

3. Results

The naturally oxidized Si membrane samples, with different thicknesses, were irradiated with a femtosecond pulsed laser ($\lambda_c = 800\,\mathrm{nm}$, $\tau = 80\,\mathrm{fs}$) at an external angle of incidence of 45 °. Both the fundamental and second harmonic (SH) signals were recorded for transmission through the membranes and reflection from the membranes as shown figure 1b.

3.1. Fundamental measurements

The beam from the oscillator is collimated, passes through a chopper of 50 % transmission and is focused by two lenses, L_1 and L_2 ($f_1 = -50\,\mathrm{mm}$ and $f_2 = 35\,\mathrm{mm}$, respectively) to diameter of ($11 \pm 2\,\mu\mathrm{m}$). The transmitted and reflected beams are collimated by lenses L_3($f_3 = 120\,\mathrm{mm}$). One power meter is used to measure the transmitted and reflected average power.

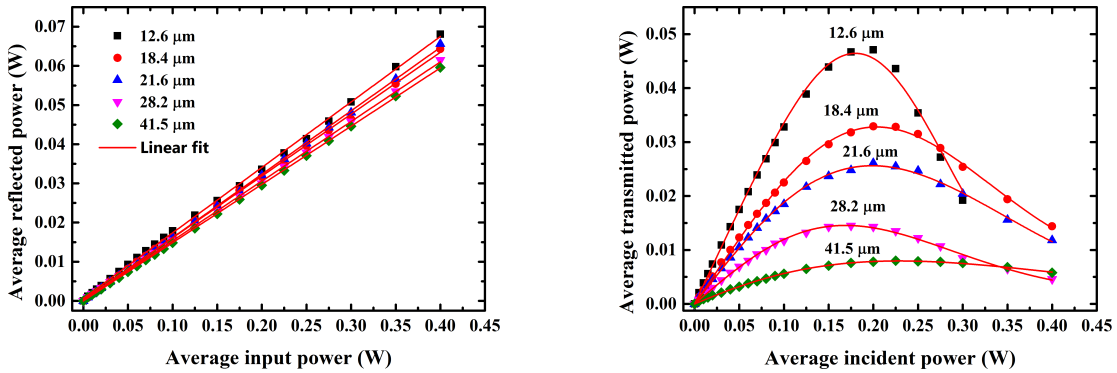

(a) (b)

Figure 2: Fundamental measurements of the average laser power reflected from (a) and transmitted through (b) a Si membranes with different thicknesses. The solid curves are fits; cf. details in the text

Figure 2 shows the results of the fundamental beam reflection from (figure 2a) and transmission through (figure 2b) Si membranes, with different thicknesses, as a function of the incident average laser power, P_{in} up to $\approx 400\,\mathrm{mW}$. For reflection, the average laser reflected power P_{re} displays a linear dependence on the incident power. This is in agreement with previous findings and confirms the validity of the Fresnel equations using the optical constants of silicon samples under ambient conditions [9]. However, the transmitted laser power P_{tr} shows a different behaviour; starting with a linear increase, it reaches a maximum around $0.15 - 0.25\,\mathrm{W}$ and decreases again as the average incident laser power is increased. Contributions from internally reflected beams to the transmitted laser power P_{tr} are negligible ($\leq$ about 2 %) because of the high reflection losses at the interfaces, even without any account for laser beam attenuation by absorption and/or scattering [12].

3.2. Time-dependent second harmonic measurements

For the time-dependent second harmonic (TDSH) generation, the p-polarized beam out of the laser (800 nm, 80 fs, 80 MHz) was incident on the Si sample, with thickness d , at an external angle 45 °. The pulse energy of the laser is < 10 nJ and the central wavelength was monitored by a spectrometer. Detection of the SH signals was made by use identical photomultiplier tubes (PMT) after blocking fundamental beams with filters.

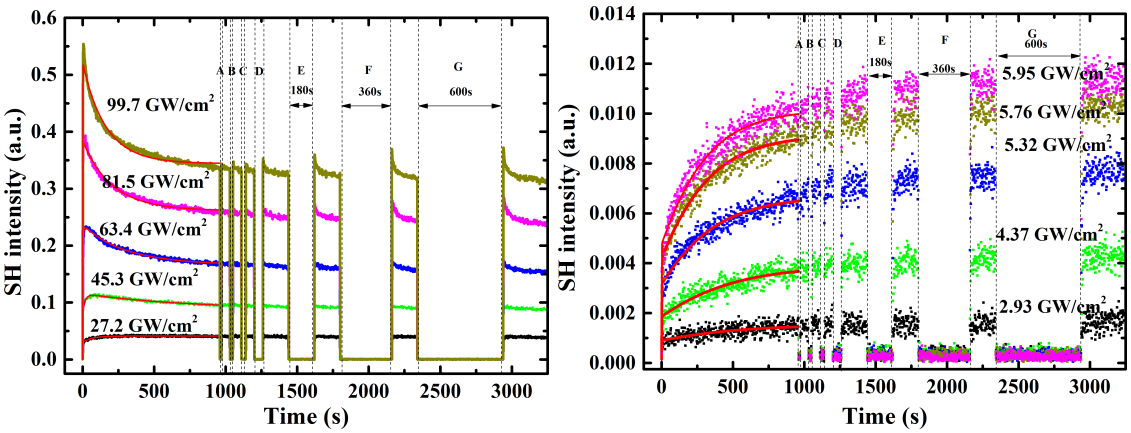

(a) (b)

Figure 3: Time-dependent second harmonic measurements in reflection (a) and in transmission (b) with dark periods: A (10 s), B (20 s), C (30 s), D (60 s), E (180 s), F (360 s) and G (600 s). The intensity value given for each curve corresponds to the local intensity of the fundamental laser beam just inside the front interface for reflections, and just inside the back interface for transmission. The membrane was $\approx 33.6\,\mu$m thick.

Figure 3 displays simultaneous measurements of second harmonic signals reflected from (figure 3a) and transmitted through (figure 3b) a silicon membrane, with thickness $d \approx 33.6\,\mu$m as a function of irradiation time, with every measurement starting on a virgin sample spot.

In reflection measurements (figure 3a), for peak intensities $\leq 27.2\,\mathrm{GW/cm^2}$, the SH signal increases on a time scale of minutes before reaching a steady state (equilibrium) up to 960 s. This effect is known as electric field induced second harmonic (EFISH) generation [11-13]. The temporal evolution can be reproduced using two exponential functions and the fit is represented by the solid curve in figure 3a. For peak intensities $> 27.2\,\mathrm{GW/cm^2}$, the SH signal show a different behaviour; first it increases on a time scale of seconds, reaches a maximum and then decreases on a time scale of minutes before reaching equilibrium. In this case the temporal evolution is reproduced using three exponential functions (see equation 3). It is observed that upon re-irradiation the SH intensity increases above the level before the dark period but less than the initial SH intensity upon onset of laser illumination. The decline after each new SH maximum occurs on a significantly shorter time scale than the slow decline after the initial maximum of the virgin sample spot.

In transmission measurements (figure 3b), the SH signal increases on a time scale of several minutes before reaching an equilibrium value. The transmitted intensities for the TDSH in transmission were calculated from the transmitted fundamental powers and correspond to the intensities listed for the reflection measurements. The dark periods seem to not affect the SH signals upon re-irradiation: the SH signal starts at the value it had when the signal was blocked.

4. Discussion and conclusion

4.1. Fundamental measurements

The absorption of Ti:sapphire laser light by slightly doped silicon membranes (in the 12 μm to 40 μm range) was investigated with a femtosecond pulsed laser. The measurements revealed a strong nonlinear power dependence of the fundamental beam transmission through the sample. The nonlinearity observed with the laser beam transmission is not attributed to photo-damage of the Si membranes because the process is reversible, i.e. it gives the same trend if the measurements start with high incident powers, but it is attributed to free carrier absorption (FCA) in silicon [13]. Laser induced sample heating and coherent two- and/or multi-photon absorption are of minor importance and can in any case not explain the observed decrease of transmitted power at high incidence powers [11]. Similar results obtained by Yamada et al. [12] with a pulsed dye laser at 590 nm irradiating a 0.6 μm thin Si layer on sapphire show a pronounced maximum followed by a lower constant transmission for further increasing input intensity. This complex transmission behaviour could nicely be fitted by a simple FCA model (equation 2 of [13])

$$\begin{aligned} I_{trans}(I_{in}, z_m) &= (I_{in} - I_c)\exp(-\alpha_1 z_m)\exp(-\alpha_{FCA} z_m) + I_c \exp(-\alpha_1 z_m) \\ &= F\left[(I_{in} - I_c)\exp(-E_n I_{in}^n) + I_c\right], \end{aligned} \tag{2}$$

where $F = \exp(-\alpha_1 z_m)$. I_c is defined as the I_0 threshold value below which electron-hole pairs are generated but do not contribute to FCA. I_{in} and I_{trans} are the average intensities just inside the front and back Si/SiO_2, respectively. α_1 is the linear absorption coefficient of Si, $z_m = d/\cos\theta$ is the optical path length in silicon with thickness d. If α_{FCA} is the FCA absorption coefficient, n_{eh} and σ_{eh} the concentration and absorption cross section of eh pairs, respectively, $\alpha_{FCA} \approx n_{eh}\sigma_{eh}$ with $n_{eh}\sigma_{eh} = \sigma_0 n_{eh}^n$ (for $n \approx 2$) [13] and $n_{eh} = \kappa I_{in}$ as the eh pairs are generated by one-photon absorption. Therefore $e^{-\alpha_{FCA} z_m} = e^{-\kappa_n z_m I_{in}^n} = e^{-E_n I_{in}^n}$. The application of equation (2) to figure 2b is shown by the solid curves. Since the original submission of this paper the model has been applied to a different dataset and values for the fitting parameters have been obtained [14]

4.2. Time-dependent second harmonic

The temporal evolution of the experimental data is reproduced, in reflection (for peak intensities $\leq 27.2\,GW/cm^2$) and in transmission geometries by fitting two exponential functions given by [15-17]. For peak intensities $> 27.2\,GW/cm^2$ (reflection), the temporal evolution of the SH response (figure 3a) cannot be explained only with electron effects. An additional effect is added to describe hole dynamics, which requires an additional two exponential functions. However, upon fitting the experimental data with four exponential functions, the fourth time constant gives unrealistic values. The experimental data were then reproduced using three exponential functions given by:

$$I^{(2\omega)}(t) \propto \sum_{i=1}^{3} \left[1 + a_i \exp(-t/\tau_i)\right]^2, \tag{3}$$

where $a_1, a_2 < 0$ and $a_3 > 0$ and $\tau_i > 0$. The time constants τ_i are dependent on the incident laser peak intensity $I_{l,p}$ [6 - 8] and follow the power law $1/\tau_i(I_{l,p}) \propto I_{l,p}^{n_i}$. In reflection geometry, for peak intensities $\leq 27.2\,GW/cm^2$, it was found that $n_1 = 2.7$ and $n_2 = 3.2$. The interpretation of these results is based on previous work done on bulk Si/SiO_2 [6], [17 - 20]. The explanation is that laser irradiation leads to electron injection and trapping in the ultrathin SiO_2 [8] and to a permanent modification of the SH response due to photoinduced trap site creation. The

superposition of electron and hole processes leads to a time-dependent EFISH signal. The energy barrier for electron injection into the SiO_2 amounts to 4.3 eV [17, 18]. Electrons surmount this interface in the bulk or at Si/SiO_2 interface by direct three-photon absorption explaining why n_1 and n_2 are close to 3 or cascade processes. For laser peak intensities $> 27.2\,GW/cm^2$ (reflection geometry), the temporal evolution of equation (3) gives the characteristic time constant τ_3, and following the power law it is found that $n_3 = 6.59$. The extracted time constant intervals are given in Table 1.

For the EFISH measurements in transmission, the extracted time constant do not follow a simple power law dependence on the incidence intensity. This would seem to indicate that FCA plays a significant role in the establishment of the interfacial electric field at the back interface. Further investigations are necessary to pinpoint this role.

Table 1: Time constants extracted from the graphs using two- and three-exponential fits

	τ_1	τ_2	τ_3
Transmission	$14 - 68\,s$	$150 - 305\,s$	
Reflection	$0.005 - 21\,s$	$0.75 - 321\,s$	$373 - 6316\,s$

In summary, the application of fs Ti: sapphire laser for the investigation of Si membrane samples in the $12\,\mu m$ to $40\,\mu m$ thickness range reveals a strong nonlinear dependence of the transmitted laser powers while the reflected powers show a linear dependence. The nonlinearity observed is attributed to FCA in Si. A FCA model (equation (2)) is used to fit the transmitted laser power data. Simultaneous measurements of the SH signals in reflection from and transmission through Si membranes show that the observed phenomena are results of the electron injection and trapping inside the ultrathin SiO_2.

5. References

[1] Helms C R and Poindexter E H 1994 *Report on Progress in Physics* **57(8)** 791
[2] Lüpke G 1999 *Surface Science Reports* **35** 75-161
[3] Lu Zhong-Yi, Nicklaw C J, Fleetwood D M, Schrimpf R D and Pantelides S T 2002 *Phys. Rev. Lett.* **89** 285505
[4] Neethling P H 2008 *Electric field induced second harmonic (EFISH) measurements of highly boron doped p^+-type Si/SiO_2*. PhD Thesis, University of Stellenbosch
[5] Nyamuda G P, Steenkamp C M, Stafast H and Rohwer E G 2011 *Appl. Phys.* B **104** 735
[6] Scheidt T, Rohwer E G, von Bergmann H M and Stafast H 2004 *European Phys. Journal : Appl. Phys.* **27** 393
[7] Scheidt T, Neethling P H, Rohwer E G, von Bergmann H M and Stafast H 2008 *Appl. Phys.* **104** 083712
[8] Scheidt T 2005 *Charge carrier dynamics and defect generation at the Si/SiO_2 interface probed by femtosecond optical second harmonic generation.* PhD Thesis, Friedrich-Schiller University Jena- Germany
[9] Sokolowski-Tinten K, Bilakowski J. D and von der Linde D. 1995 *Phys. Rev. B* **51** 14186
[10] Bing Gu and Jing Chen and Ya-Xian Fan and Jianping Ding and Hui-Tian Wang 2005 *J. Opt. Soc. Am. B* **22** 2651–2659
[11] Mihaychuk J C, Bloch J and van Driel H M 1995 *Opt. Lett.* **20** 2063
[12] Yamada M, Kotani H, Yamamoto K and Abe K 1981 *Phys. Lett.* **85A** 191
[13] Heisel P -C, Ndebeka W I, Neethling P H, Paa W, Rohwer E G, Steenkamp C M and Stafast H 2016 *Appl. Phys. B: Lasers and Optics* **122** 60
[14] Ndebeka W I, and Neethling P H, and Steenkamp C M, and Bergmann J, and Rohwer E G and Stafast H. June 2016 Interband and free charge carrier absorption in silicon at 800 nm: experiments and model calculations, manuscript in preparation
[15] Aktsipetrov O A, Fedyanin A A, Golovkina V N and Murzina T V 1994 *Opt. Lett.* **19** 1450
[16] Bloch J, Mihaychuk J G and van Driel H M 1996 *Phys. Rev. Lett.* **77** 620
[17] Mihaychuk J G, Shamir N and van Driel H M 1999 *Phys. Rev.* B **59** 2164
[18] Cernusca M, Heer R and Reider G A 1998 *Appl. Phys. B: Lasers and Opt* B **66** 367
[19] Balk P 1988 *Material Science Monographs* **32**
[20] Scheidt T, Rohwer E G, von Bergmann H M and Stafast H 2004 *Phys. Rev. B* **69** 155314